IBRACON Structures and Materials Journal
Revista IBRACON de Estruturas e Materiais
ISSN 1983-4195 ismj.org

ORIGINAL ARTICLE

Durability of binary geopolymers with metakaolin and porcelain polishing residue against magnesium sulfate attack

Durabilidade de geopolímeros binários com metacaulim e resíduo de polimento de porcelana frente ao ataque por sulfato de magnésio

Giovanny Antonio Ramos[a]
Rafael Dors Sakata[b]
Laura Silvestro[c]
Carlos Eduardo Maduro de Campos[d]
Fernando Pelisser[a]

[a]Universidade Federal de Santa Catarina – UFSC, Departamento de Engenharia Civil, Laboratório de Aplicações de Nanotecnologia em Construção Civil – LabNANOTEC, Florianópolis, SC, Brasil
[b]Universidade Tecnológica Federal do Paraná – Paraná – UTFPR, Curitiba, PR, Brasil
[c]Universidade Tecnológica Federal do Paraná – Paraná – UTFPR, Coordenação do Curso de Engenharia Civil, Guarapuava, PR, Brasil
[d]Universidade Federal de Santa Catarina – UFSC, Departamento de Física, Laboratório de Difração de Raios X – LDRX, Florianópolis, SC, Brasil

Received 20 January 2025
Revised 30 July 2025
Accepted 01 September 2025

Abstract: Geopolymers are emerging as alternative binders capable of incorporating various residual materials. However, further research is needed to assess the durability of these systems. This study produced geopolymer pastes with metakaolin (MK) partially replaced by porcelain polishing residue (PPR) at levels ranging from 0 to 45% by weight. The performance of these pastes was evaluated under magnesium sulfate attack over a 90-day period, using compressive strength tests, FTIR, TGA, and quantitative X-ray diffraction analyses (QXRD). Increases in compressive strength of up to 23% were observed after exposure to magnesium sulfate (30N1S1 and 45N1S1), with a similar trend across all levels of MK replacement by RPP, when compared to their respective reference samples not exposed to sulfate attack. This trend is likely related to the absence of expansive products commonly linked to sulfate attacks, such as ettringite and gypsum, as confirmed by XRD. Moreover, the SEM-EDS analysis suggests the incorporation of magnesium ions (Mg2+) into the matrix, which bond with the aluminosilicate gel, enhances its performance. These findings highlight the potential of MK and PPR-based geopolymeric materials for use in sulfate-aggressive environments, contributing to the advancement and sustainability of the construction industry.

Keywords: geopolymer, durability, sulfate, porcelain polishing residue.

Resumo: Geopolímeros têm emergido como ligantes alternativos capazes de incorporar diversos materiais residuais. No entanto, ainda são necessárias pesquisas adicionais para avaliar a durabilidade desses sistemas. Neste estudo, foram produzidas pastas geopoliméricas com metacaulim (MK) parcialmente substituído por resíduo de polimento de porcelanato (RPP) em níveis variando de 0 a 45% em massa. O desempenho dessas pastas foi avaliado frente ao ataque por sulfato de magnésio durante um período de 90 dias, por meio de ensaios de resistência à compressão, FTIR, TGA e análises de difração de raios-X quantitativa (QXRD). Foram observados aumentos de resistência à compressão de até 23% após a exposição ao sulfato de magnésio (30N1S1 e 45N1S1), com tendência semelhante em todos os níveis de substituição de MK por RPP, quando comparados às respectivas amostras de referência não expostas ao ataque por sulfato. Essa tendência provavelmente está relacionada à ausência de produtos expansivos comumente associados ao ataque por sulfatos, como etringita e gipsita, conforme confirmado por DRX. Além disso, a análise por MEV-EDS sugere que a incorporação de íons de magnésio (Mg^{2+}) à matriz, os quais se ligam ao gel aluminosilicato, melhora o seu desempenho. Esses resultados destacam o potencial dos materiais geopoliméricos à base de MK e RPP para aplicação em ambientes agressivos a sulfatos, contribuindo para o avanço e a sustentabilidade da indústria da construção.

Palavras-chave: geopolímero, durabilidade, sulfato, resíduo de polimento de porcelanato.

Corresponding author: Fernando Pelisser. E-mail: f.pelisser@ufsc.br
Financial support: The authors acknowledged the Brazilian research agencies National Council for Scientific and Technological Development (CNPq), Coordination for the Improvement of Higher Education Personnel (CAPES), and Santa Catarina Research Foundation (FAPESC).
Conflict of interest: Nothing to declare.
Data Availability: The data that support the findings of this study are available from the corresponding author, Fernando Pelisser, upon reasonable request.

This is an Open Access article distributed under the terms of the Creative Commons Attribution license (https://creativecommons.org/licenses/by/4.0/), which permits unrestricted use, distribution, and reproduction in any medium, provided the original work

How to cite: G. A. Ramos, R. D. Sakata, L. Silvestro, C. E. M. Campos, and F. Pelisser, "Durability of binary geopolymers with metakaolin and porcelain polishing residue against magnesium sulfate attack," *Rev. IBRACON Estrut. Mater.*, vol. 18, no. 5, e18501, 2025, https://doi.org/10.1590/S1983-41952025000500001.

1 INTRODUCTION

Cement is the most widely produced material globally [1] and is responsible for approximately 5% of the world's carbon dioxide (CO_2) equivalent greenhouse gas emissions [2]. Forecasts indicate an increase in cement consumption due to population growth and demand for infrastructure in developing countries [3], [4]. However, studies report the occurrence of early deterioration in cement-based materials, especially in chemically aggressive environments [5], [6]. In sewage treatment plants, for example, there is direct contact with sulfates and aggressive acids from decomposing organic matter [7]–[9]. In marine environments, saline and alkaline regions, sulfate attacks are among the main agents of degradation of infrastructure works [10], [11]. In addition, it also occurs due to sulfates and sulfides existing in the aggregates used in the composition of concrete [12]. Acid attacks are usually caused by acid rain or industrial environments, such as automotive batteries, and fertilizers [13].

Ordinary Portland cement (OPC) has intrinsic limitations in resisting chemical attack due to the high calcium content in its composition. The poor performance of OPC against sulfate attack can be attributed to (i) the high solubility and leaching of calcium hydroxide, which reduces the alkalinity of the matrix, and (ii) the formation of expansive ettringite crystals. Additionally, magnesium sulfate attack has been identified as the most detrimental to the durability of OPC-based materials [14]. Thus, using alternative binders with satisfactory chemical attack resistance is relevant. The geopolymers demonstrated high durability against acid [15], [16] and sulfate attack [17], [18]. Nonetheless, the systematic literature review of articles in the Scopus database presented in Figure 1 revealed that microstructural analysis remains an underexplored topic in durability geopolymer studies, emphasizing opportunities for further research.

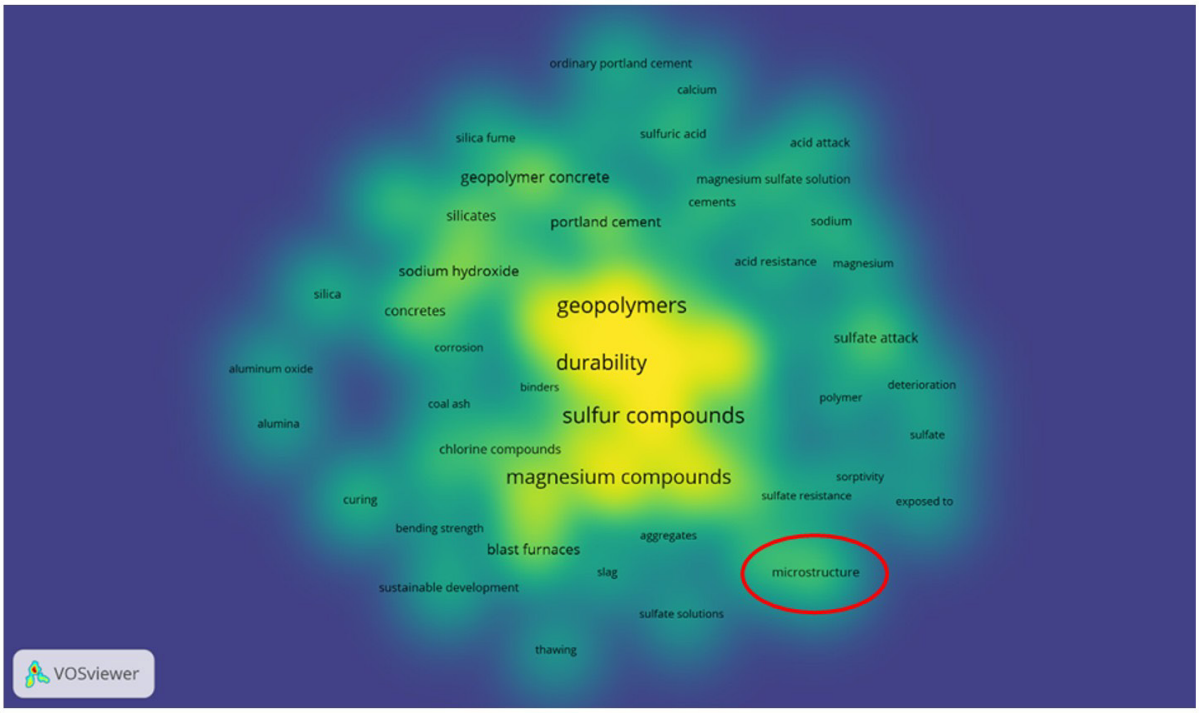

Figure 1. Density map of keywords from studies using the following search terms: 'geopolymer' AND 'durability' AND 'sulfate' AND 'magnesium' in the title, keywords, and abstract. Search conducted on the Scopus platform on August 22, 2024.

Cation exchange with the sulfate solution occurs in geopolymers with low or no calcium content, forming an N-A-S-H structure more resistant to sulfate attack. This enhanced resistance is due to the reduced formation of crystalline phases typically associated with expansion in OPC materials, such as ettringite, gypsum, and thaumasite [19]. Elyamany et al. [20]

investigated the effects of curing temperature, sodium hydroxide solution molarity, alkaline solution-to-binder ratio, and binder type on the magnesium sulfate resistance of geopolymer mortar, with comparisons made to OPC mortar. The study found that geopolymer mortars exhibited superior resistance to magnesium sulfate compared to OPC mortars. Additionally, increasing the curing temperature and sodium hydroxide solution molarity and decreasing the alkaline solution-to-binder ratio further enhanced the magnesium sulfate resistance of geopolymer mortars.

Deng and Deng [21] evaluated the durability of ternary geopolymers composed of granulated blast-furnace slag (GBFS) and fly ash (FA), reinforced with polyvinyl alcohol (PVA) fibers, under magnesium sulfate exposure for up to 90 days. A slight increase in compressive strength (5–8%) was observed after sulfate exposure, which could be attributed to (i) the formation of sodium-calcium-magnesium sulfo-aluminosilicate crystals, leading to reduced porosity in the geopolymer; (ii) the presence of only small amounts of expansive gypsum and ettringite crystals; and (iii) enhanced stability and increased mean chain length of aluminosilicate polymer structures. Conversely, Singh et al. [22] observed reductions in residual compressive strength, ranging from 10.3% to 21.7%, after up to 180 days of exposure to magnesium sulfate solution in geopolymer concretes made with varying proportions of GBFS, fly ash (FA), and silica fume (SF), and incorporating both natural and 100% recycled coarse aggregates (RCA). OPC concretes, composed of natural and RCA, exhibited residual compressive strength reductions of 28.2% and 33.4%, respectively.

Beltrame et al. [23] evaluated the resistance of metakaolin-based geopolymeric mortars to sodium and magnesium sulfate attack over 20 weeks, considering different activator compositions and the use of an air-entraining admixture. Mortars with higher sodium silicate content exhibited greater expansion and deterioration. SEM/EDS analyses revealed the formation of M-A-S-(H) gels and caminite in $MgSO_4$ exposure. Overall, the compositions maintained compressive strength after $MgSO_4$ exposure. Moreover, the air-entraining admixture was ineffective in mitigating the stresses induced by sulfate attack. Trisotto et al. [24] investigated the sulfate resistance of metakaolin-based geopolymer concretes, varying Na_2O content, curing conditions, and water/metakaolin ratios. After 10 weeks of exposure to sodium and magnesium sulfates, results indicated that sodium sulfate caused significantly more damage compared to magnesium sulfate.

Therefore, while the literature typically indicates that geopolymers offer superior performance against magnesium sulfate compared to OPC-based materials, there is considerable variability in the reported results, particularly concerning exposure duration and geopolymer composition. This highlights the need for further research, particularly involving alternative residual or waste precursors beyond the commonly used ones, such as GBFS and FA. Future studies should emphasize detailed mineralogical and microstructural analyses, the phases consumed, and products formed during interactions with magnesium sulfate solutions.

Geopolymers are inorganic polymers obtained through alkaline activation of amorphous or partially amorphous aluminosilicates [25]. In addition to resistance to chemical attack, geopolymers can provide high mechanical strength and fire resistance [26], good workability [27], and the ability to encapsulate toxic elements [28], [29]. An environmental advantage is due to the possibility of being produced using a wide variety of raw materials, including waste and industrial by-products, such as fly ash [15]–[17], heavy ash [30], red mud [31], glass dust from fluorescent lamps [32], wood [33] and oat husk [34] ashes, among others, such as porcelain polishing residue (PPR) [35], used in this research.

During the polishing of porcelain tiles using metallic brushes, the resulting by-product comprises both the polished ceramic material and the metallic abrasives. This contamination by abrasives renders the by-product unsuitable for reintegration into the production process, as the abrasive components in the PPR can cause deformations in the ceramic pieces during firing. Then, the PPR starts to be deposited in controlled landfills since it does not have an established reuse. However, research on this topic is scarce. Ramos et al. [35] evaluated the effect of incorporating PPR into geopolymer pastes, having obtained an increase in mechanical performance in one of the studied compositions. Further, Ramos et al. [27] found that using this waste favors the workability of geopolymers and reduces the carbon footprint in terms of CO2 equivalent emissions. However, to the best of the authors' knowledge, there is a knowledge gap regarding the performance of geopolymeric compositions made with metakaolin and PPR under magnesium sulfate attack. Thus, the present work aimed to study the influence of the incorporation of PPR and the concentration of the alkaline activator in metakaolin-based geopolymer cement pastes subjected to the action of magnesium sulfate under conditions of accelerated exposure through the evaluation of compressive strength and microstructural and mineralogical tests.

2 EXPERIMENTAL PROCEDURE

2.1 Materials

PPR was collected from a company specializing in surface polishing ceramic tiles in southern Brazil. It was collected with about 30% humidity, dried at 60 °C until constant weight, and had a density of 2.48 g/cm^3 and a mean particle diameter of 13.7 μm. A commercial metakaolin (MK) was also employed, with a density of 2.56 g/cm^3 and a mean

particle diameter of 9.3 µm. Figure 2 shows PPR and MK's particle size distribution (PSD). The chemical composition of PPR and MK are shown in Table 1. Sodium hydroxide (*Neon*™) with a purity of > 99% and density of 2.12 g/cm^3 and sodium silicate solution (Manchester™) composed of 8.2% Na_2O, 27.5% SiO_2, and 64.3% H_2O by weight and density of 1.50 g/cm^3 were used as alkaline activators.

Table 1. Chemical composition of MK and PPR.

Oxide (wt.%)	MK	PPR
SiO_2	54.00	67.70
Al_2O_3	42.00	21.00
Fe_2O_3	0.50	1.80
TiO_2	0.50	0.70
CaO	0.10	2.60
MgO	0.10	1.10
K_2O	0.50	2.30
Na_2O	0.10	1.80
ZrO_2	-	0.30
Loss on ignition	2.00	0.80

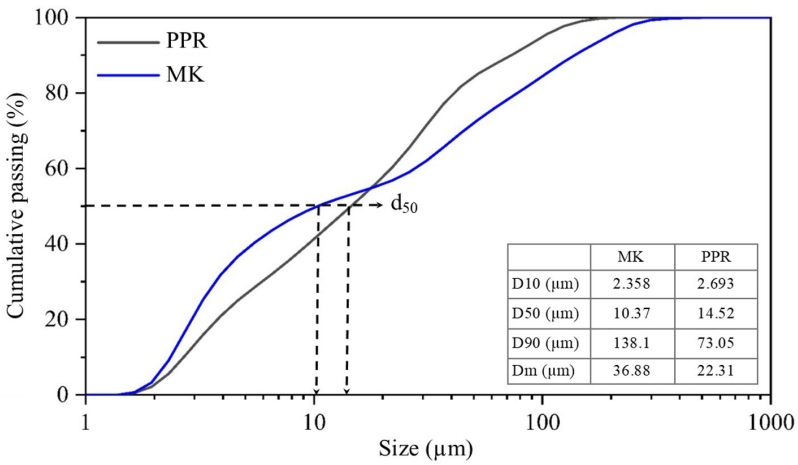

Figure 2. Particle size distribution of MK and PPR.

Figure 3 shows the X-ray diffraction (XRD) patterns of the precursors (MK and PPR) materials, obtained using an X' Pert Pro (*PANalytical*™) diffractometer operated at 45 kV and 40 mA acceleration voltage and CuKα incident radiation with λ = 1.518 Å. The scanning ranged from 7 to 70° 2θ; the step size was 0.0167° 2θ with a cumulative scanning time of 60 min. The samples were rotated at 2 s/rev. The main crystalline phase found in both materials was quartz. In addition, MK showed ilite, kaolinite, and microcline peaks, while PPR showed albite and mullite peaks. Finally, MK and PPR presented a hump at 2θ from 5 to 45°, indicating the presence of amorphous structures in both materials. Table 2 provides the mineralogical composition of the materials used in this study, including the amorphous content determined by the PONCKS method [36]. MK has a higher amorphous content than PPR, which will impact the precursor's reactivity, as discussed in the results section. Additionally, approximately 7.0% kaolinite in MK suggests that the calcination temperature may have been suboptimal.

2.2 Specimen Preparation

Pastes were prepared with 0-45 wt.% partial replacement of MK by PPR. The details of each evaluated composition are in Table 3 on a weight basis and Table 4 on a molar basis (considering the total composition of precursors, i.e., amorphous and crystalline portions). The proportions were determined based on the study performed by Ramos et al. [35]. The alkaline activator was initially prepared by dissolving the NaOH flakes into the Na_2SiO_3 solution. After mixing, the samples were cast into plastic molds, sealed, vibrated, and cured in a stove at 23°C for 28 days.

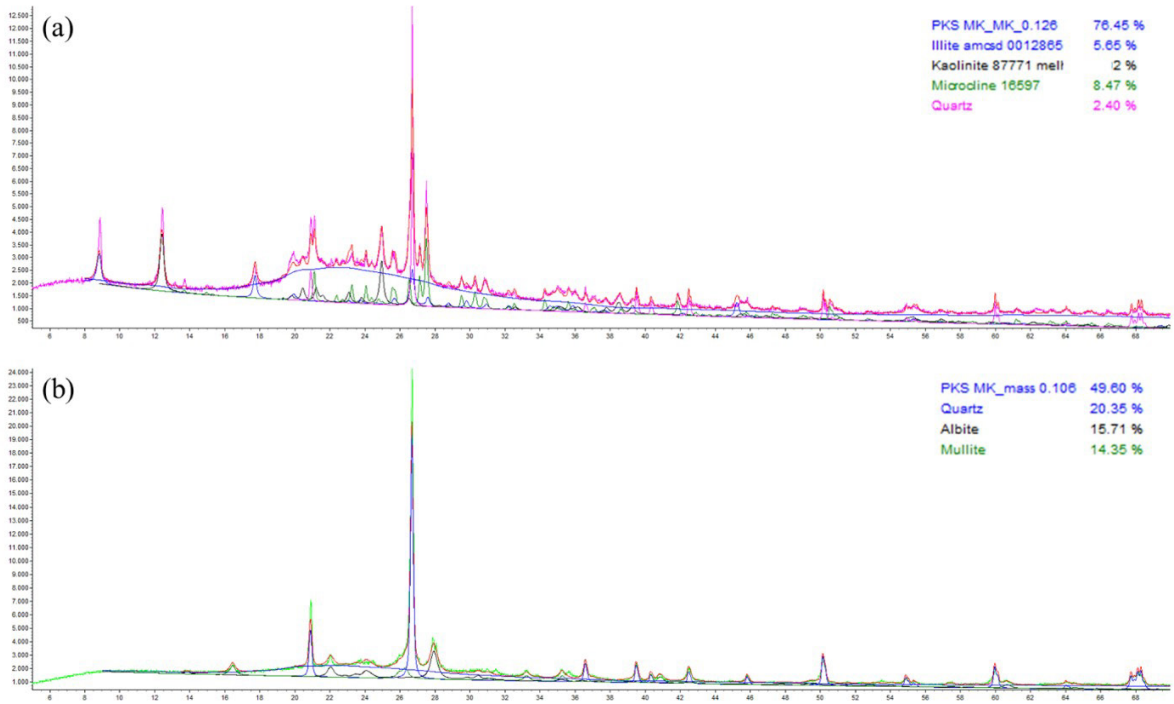

Figure 3. XRD pattern of (a) MK and (b) PPR. Note: The colors assigned to each phase in the diffractograms correspond to the peaks of the respective phases illustrated in the figure.

Table 2. Mineralogical composition of MK and PPR determined by XRD.

Mineral	MK (%)	PPR (%)
Albite	-	14.35
Mullite	-	15.71
Illite	5.65	-
Kaolinite	7.02	-
Microcline	8.47	-
Quartz	2.40	20.35
Amorphous (PONCKS)	76.45	49.60

Table 3. Composition of the geopolymer pastes on a weight basis.

Composition	PPR (%)	MK (%)	Na_2SiO_3 (%)	NaOH (%)
0n1s1	0.0	46.9	47.9	5.2
15n1s1	7.0	39.8	47.9	5.2
30n1s1	14.1	32.8	47.9	5.2
45n1s1	21.1	25.8	47.9	5.2
0n2s2	0.0	44.6	49.5	5.9
15n2s2	6.7	37.9	49.5	5.9
30n2s2	13.4	31.2	49.5	5.9
45n2s2	20.0	24.5	49.5	5.9

Note: the nomenclature used refers to the percentage of MK replacement by RCP in the first number (xx-n1s1), while "n1s1" and "n2s2" refer to the composition of the activating solution used.

2.3 Experimental methods

The durability of samples exposed to sulfate attack was evaluated using a range of characterization techniques: visual inspection, X-ray diffraction (XRD), Fourier transform infrared spectroscopy (FTIR), scanning electron microscopy (SEM) coupled with energy-dispersive X-ray spectroscopy (EDS), and thermogravimetric analysis (TGA).

Additionally, compressive strength was assessed before and after exposure to magnesium sulfate. XRD and FTIR analyses were conducted on the same specimen's center and edge (Figure 4), while SEM/EDS and TGA analyses were focused on the edge. Cylindrical specimens (24 mm in diameter and 28 mm in height) were used for the tests. The sulfate attack procedure involved immersing the specimens, after 28 days of hydration, in a 5.0 wt.% magnesium sulfate solution [22], [37], [38], with mechanical and microstructural/mineralogical properties evaluated after 30, 60, and 90 days of exposure.

Table 4. Molar ratio of the as-prepared compositions of the geopolymeric system.

Composition	SiO_2/Al_2O_3	SiO_2/Na_2O	Na_2O/SiO_2	$Na_2SiO_3/NaOH$
0n1s1	3.37	9.73	0.35	1.08
15n1s1	3.73	9.69	0.39	1.08
30n1s1	4.16	9.65	0.43	1.08
45n1s1	4.67	9.62	0.49	1.08
0n2s2	3.47	9.24	0.38	0.98
15n2s2	3.84	9.21	0.42	0.98
30n2s2	4.28	9.19	0.47	0.98
45n2s2	4.80	9.17	0.52	0.98

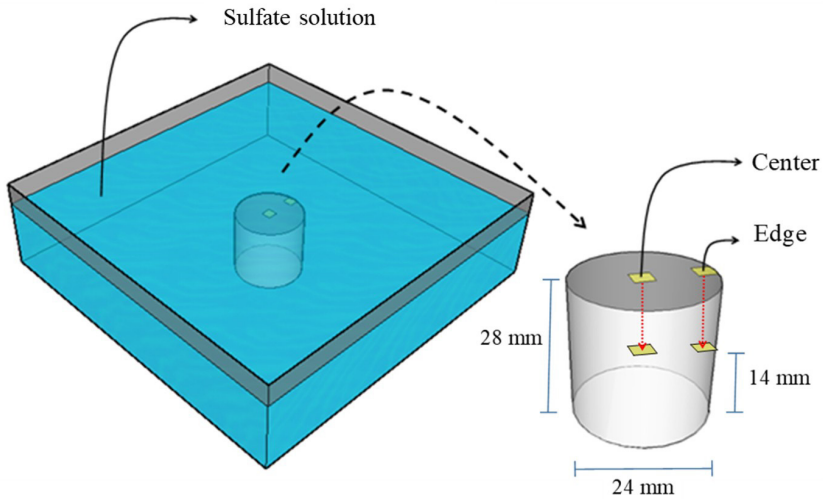

Figure 4. Illustration of specimen portions selected for XRD and FT-IR analysis.

To perform the FTIR, XRD, and TGA analysis, the specimens were dried in an oven until mass constancy (5 days in vacuum desiccator), ground in a ball mill for 10 min, and sieved through a 75 mm sieve. FTIR analysis was performed in an FT/IR-4200 (*Jasco*™) spectrophotometer in transmittance mode (0.4 cm/s scanning rate and 4000 to 400 cm^{-1} interval). XRD analysis using a X' Pert Pro (*PANalytical*™) diffractometer (2θ from 7 to 70°, 45 kV and 40 mA acceleration voltage and CuKα 1.2 incident radiation with λ = 1.518 Å). TGA analysis was performed on the SDT-Q600 (*TA Instruments*™), simultaneously performing differential thermal analysis and thermogravimetry, with atmosphere control using nitrogen gas (temperature range 23-1000 °C, heating rate of 20 °C/min). A compressive strength test was conducted according to ASTM C1231/C1231M [39] in an electrohydraulic machine (INSTRON) at 0.5 MPa/s loading rate, testing three replicates for each composition.

2.3.1. Quantitative XRD analysis

Quantitative analyses of the phases were performed using the Rietveld method, the software TOPAS v5 (Bruker™), and the Inorganic Crystal Structure Database (ICSD) from the American Mineralogist Crystal Structure Database (AMCSD). The background (2^o order Chebyshev polynomial and 1/2θ term) and the sample displacement were the global parameters refined.

The internal standard method was used to determine the amorphous content of the PPR and MK, and 10 wt.% corundum (α-Al_2O_3) was mixed as an internal standard. The PPR and MK amorphous fraction was modeled with tetragonal P4 (space group n. 75) hkl phases and quantified with the PONKCS method. The amorphous fraction of the NASH was modeled with Orthorhombic F2dd (space group n. 43) hkl phases on a well reacted geopolymer; this model fitted on the studied geopolymers with R_{wp} index lower than 7% for all refinements. The external standard method [40] was used to quantify the geopolymer MK and crystalline phases. To quantify the NASH phase, it was considered that the difference between the sum of the other phases and 100% was the amount of N-A-S-H.

The Weighted Profile R-factor (Rwp) (Equation 1) evaluated the analyses' quality. Amorphous portions of aluminosilicates (MK and PPR) unreacted during geopolymerization and the reaction product (N-A-S-H gel) were quantified by the PONKCS method (Partial or no Know Crystal Structure), described by Scarlett and Madsen [41]. Diffuse scattering signals from amorphous phases were refined using Pawley's curve fitting algorithm.

$$R_{wp} = 100 \times \left\{ \frac{\sum_i^n w_i \, [y_i(obs) - y_i(calc)]^2}{\sum_i^n w_i \, [y_i(obs)]^2} \right\}^{1/2} \quad (1)$$

where $w_i = \frac{1}{\sqrt{y_{obs}}}$ is static weight function, $y_i(obs)$ count observed in the ith step; $y_i(calc)$ is count calculated in the ith step.

3 RESULTS AND DISCUSSION

3.1 Visual Analysis

Figure 5 provides a qualitative visual assessment of the specimens' appearance following exposure to the magnesium sulfate solution at 90 days - and the reference specimens not exposed to the sulfate solution. The images reveal no noticeable surface alterations, irrespective of the MK replacement level by PPR or the geopolymer compositions evaluated. Furthermore, no cracks were detected in the specimens, which might have indicated no formation of expansive products commonly linked to sulfate attack. Additionally, Zerzouri Lakhssassi et al. [42] reported that FA-based geopolymer specimens developed superficial efflorescence after exposure to a magnesium sulfate solution, a phenomenon not observed in the present study. These findings suggest that the geopolymeric compositions exhibit robust performance, a topic that will be explored in greater detail in the subsequent sections. For OPC-based matrices, Makhloufi et al. [43] observed the formation of a thin white layer on the surface of quaternary cement specimens (comprising OPC, limestone filler, GBFS, and natural pozzolan with a volcanic origin). This layer is attributed to the formation of gypsum, followed by the dissolution of portlandite and the progressive decalcification of C-S-H and sulfoaluminate phases, especially ettringite. Sirisawat et al. [44] further note that the surface deterioration of OPC-based materials is so severe that it becomes challenging to prepare the surfaces for compressive testing and accurately estimate the cross-sectional area needed for compressive strength calculations.

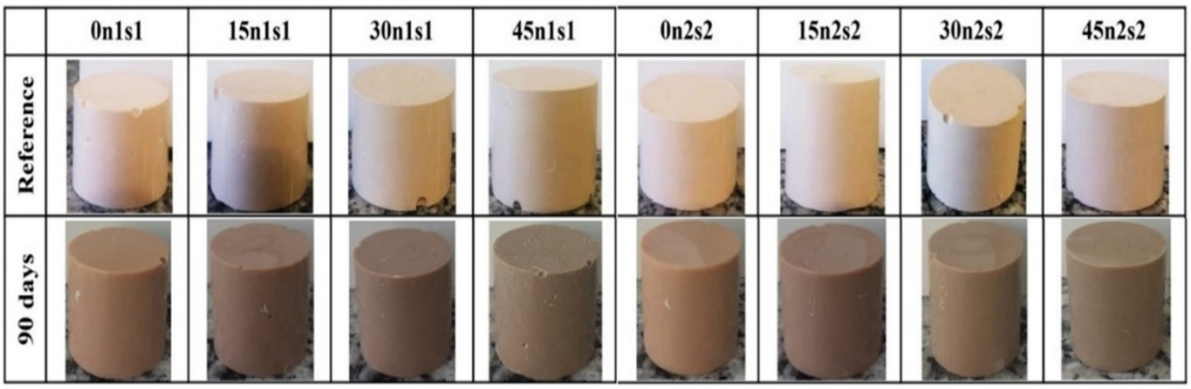

Figure 5. Visual analysis of geopolymer before and after being submitted to sulfate attack for 90 days.

3.2 Microstructural Analysis

3.2.1 FTIR

Figure 6 and Figure 7 show the FTIR results of geopolymer samples after 30 and 90 days of exposure to magnesium sulfate solution for n1s1 and n2s2 groups, respectively. Overall, the band located at ~3440 cm^{-1} and ~1640 cm^{-1} are assigned to stretching vibrations of O-H and H-O-H bonds of water molecules, whether it is the ambient humidity affecting the sample analysis or the water present in the N-A-S-H gel [45], [46]. The band at 1420 cm^{-1} corresponds to the stretching vibrations of C-O-C. It indicates the presence of carbonyl groups (CO_3^{2-}) related to the carbonation of the system that forms sodium carbonate [47].

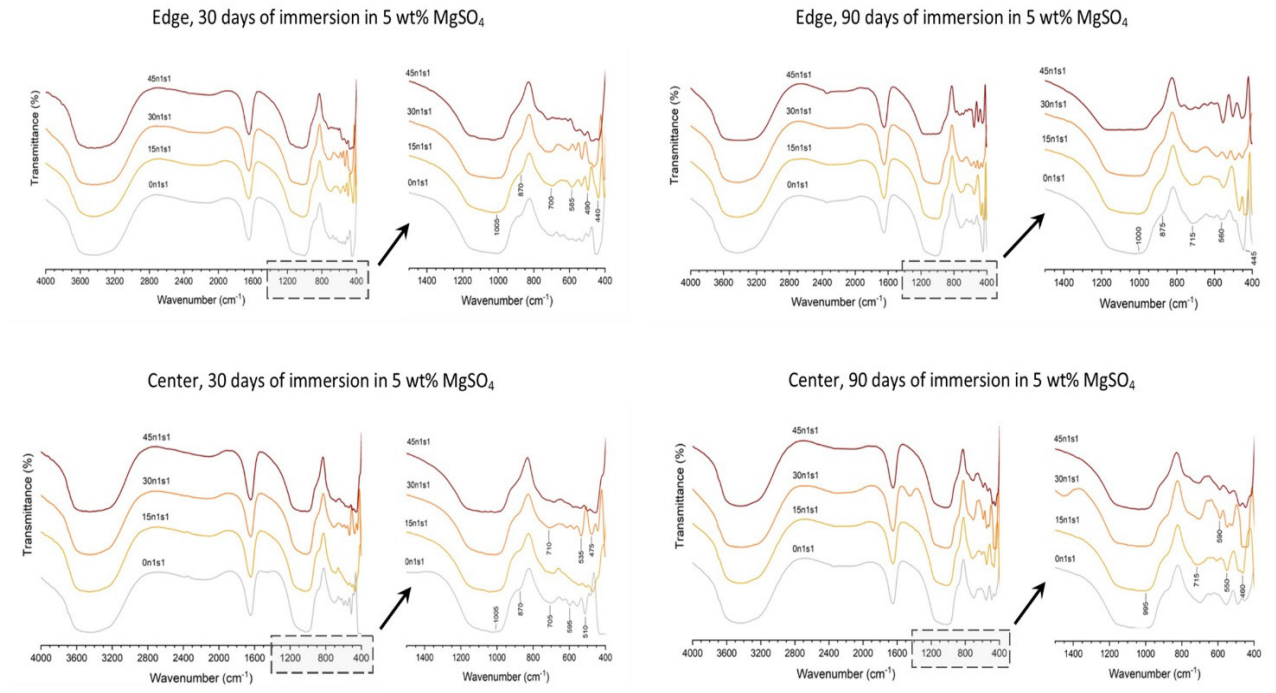

Figure 6. FTIR spectra of n1s1 group geopolymers submitted to sulfate attack for the two immersion ages (30 and 90 days) and in the two positions of the specimen (edge/center).

In geopolymers exposed to sulfate attack, the FTIR spectra revealed minimal changes, consistent with findings from other studies [13], [17], [18]. Overall, sulfate exposure slightly reduced the peak intensity of water and H-O-H bonding at the 1650 cm^{-1} band. Additionally, sulfate attack diminished the peak associated with carbonate at 1420 cm^{-1}, which was completely eliminated in samples subjected to prolonged exposure, particularly at the edges. However, it is crucial to acknowledge that sample preparation and environmental exposure can significantly affect the bands related to water and carbonate, complicating FTIR analysis due to these external interferences.

Furthermore, in the low-frequency bands located between 500 and 600 cm^{-1}, small variations in the spectra associated with double ring vibrations were identified, similar to what was found by Bakharev [17], having been considered by the author as insignificant variations. Specifically regarding the edge samples, it was observed that the ~1000 cm^{-1} band, related to the Si-O-Al bond, associated with the N-A-S-H gel, showed a small intensification in its peak, without changing its displacement according to also found by Kwasny et al. [13].

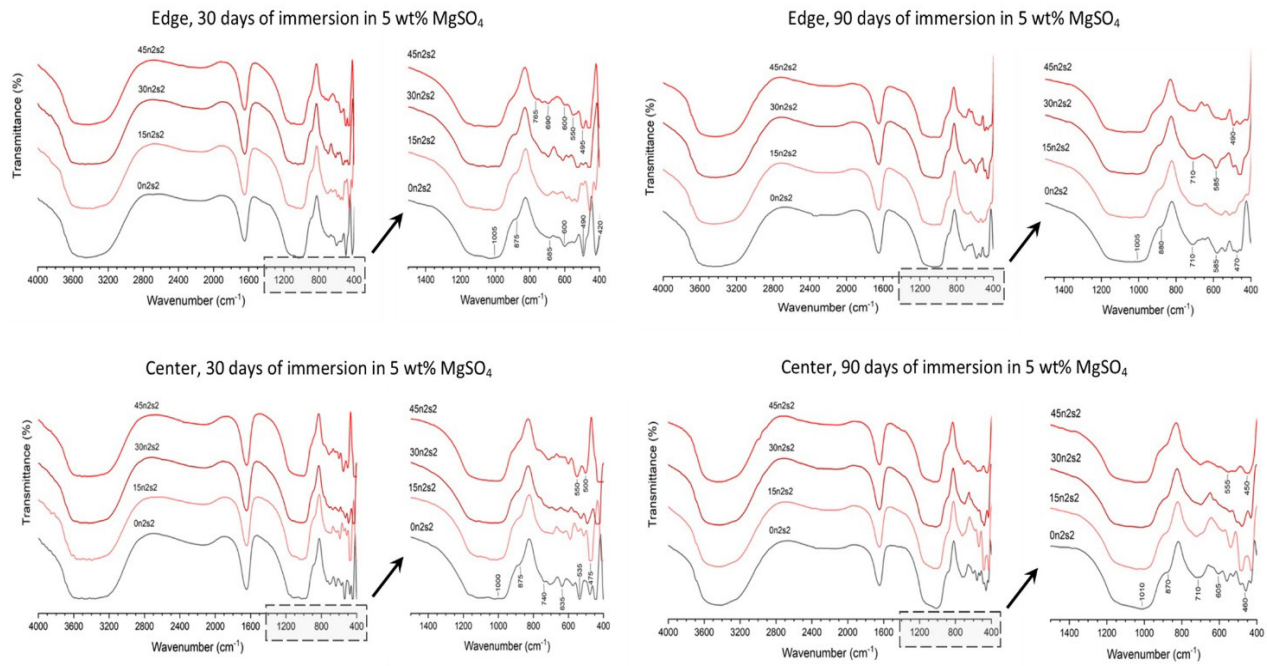

Figure 7. FTIR spectra of n2s2 group geopolymers submitted to sulfate attack for the two immersion ages (30 and 90 days) and in the two positions of the specimen (edge/center).

3.2.2 Quantitative XRD

Overall, the crystalline phases identified in MK-based geopolymers were quartz, illite, kaolinite, and microcline. Albite and mullite were also found for MK and PPR-based geopolymers. These phases are consistent with the precursor composition previously presented (Figure 3). By the PONCKS methodology, the amorphous/non-crystalline percentages, relative to unreacted aluminosilicate (MK and PPR) and the N-A-S-H gel, could be quantified. Thus, associating these phases with the Rietveld method, the samples showed a satisfactory degree of fit, with a weighted profile factor of less than 6.7%, in all diffractograms of the geopolymers. The immersion in magnesium sulfate for 90 days did not show significant differentiation in the quantified phases between the central portion of the specimen and its edge - even though the latter was more exposed to the action of the chemical agent, indicating that the sulfate percolated up to the central portion (Table 5). This trend could be expected due to the small dimensions of specimens and the exposure time assessed.

Table 5. Variation of the percentages quantified by Rietveld-PONCKS due to the chemical attack for the 15n1s1 sample.

Phases	Without sulfate exposure	Sulfate – 90 days	
		Edge	Center
Albite	1.8%	2.0%	2.1%
Mulite	1.0%	1.4%	1.1%
Quartzo	3.1%	3.6%	4.0%
Ilite	5.0%	4.4%	4.3%
Kaolinite	3.1%	2.8%	2.8%
Microcline	5.0%	3.4%	3.3%
Aluminossilicate (PONCKS)	10.2%	24.9%	23.8%
N-A-S-H experimental (PONCKS)	70.7%	57.5%	58.5%

Figure 8 presents the percentages of N-A-S-H gel calculated using the Rietveld-PONCKS method for the samples before contact with the magnesium sulfate solution and after 90 days of exposure (at the edge and center of the specimens, as illustrated in Figure 4). Notably, the progressive replacement of MK with PPR did not result in significant changes in the N-A-S-H content for both evaluated groups, specifically n1s1 and n2s2. For the n1s1 data set, equivalent

N-A-S-H percentages were observed for PPR contents of 15% (15n1s1) and 30% (30n1s1). For the 45n1s1 composition, a slight reduction of only 6.5% was observed, which may fall within the variability of the quantification method. Within the n2s2 group, reductions of approximately 11.2% (30n2s2) and 12.5% (45n2s2) were observed compared to the reference composition (0n2s2). These slight reductions are consistent with expectations, as PPR's reactivity and amorphous content are lower than those of the reference precursor, metakaolin, as detailed in the Materials and Methods section (Table 2). This behavior also explains the decreases in compressive strength of the geopolymeric matrices with increasing substitution of MK with PPR, as presented in section 3.2.5. Ramos et al. [35] also observed that higher PPR content in geopolymers containing MK and PPR led to reduced amorphous halos in the XRD patterns, indicating a decrease in hydration products resulting from the geopolymeric reactions.

The XRD results from samples exposed to the magnesium sulfate attack showed that, regardless of the PPR replacement content and the percentage of alkaline activator, all samples experienced a reduction in N-A-S-H content after 90 days of exposure compared to their respective reference subgroups. Moreover, a trend of more substantial reductions in the N-A-S-H gel percentage was observed with increasing MK replacement by PPR, with reductions of approximately 18.0% (15% PPR), 22.0% (30% PPR), and 30.0% (45% PPR). However, even with a reduction in N-A-S-H content after exposure to the sulfate solution, the geopolymer samples showed increases in compressive strength (see section 3.2.5). This can be partly attributed to the lack of expansive phases, such as ettringite, gypsum, or thaumasite, commonly found in OPC samples exposed to sulfate attack [19].

After sulfate exposure, Song et al. [48] reported similar findings in geopolymer concrete containing red mud and MK. They attributed the enhanced sulfate resistance of geopolymers, compared to OPC, to the inert interaction between sulfates and the hydration products of geopolymers. While OPC concrete exhibited expansion damage from ettringite and gypsum, geopolymer was characterized by sodium sulfate crystals and showed no signs of expansion products [48].

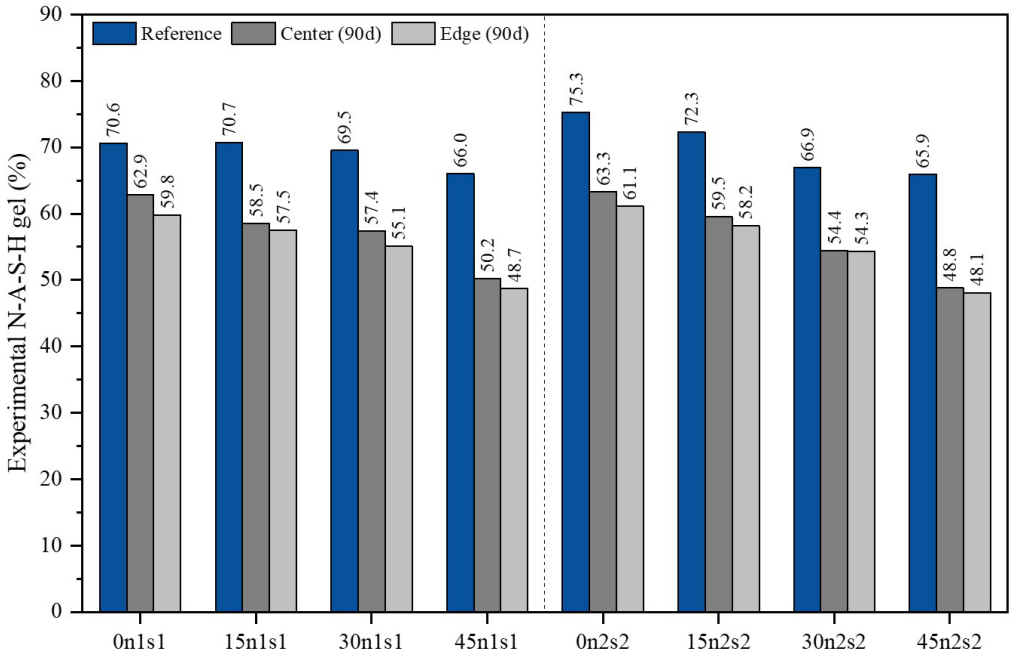

Figure 8. Variation of experimental N-A-S-H gel in geopolymers submitted to sulfate attack.

3.2.3 SEM-EDS

Figure 9 and Figure 10 show two examples of micrographs and EDS analysis of the sample without residue (0n1s1) and with 30% PPR (30n1s1), immersed in 5 wt% magnesium sulfate attack for 90 days, and the reference geopolymer (unexposed). A slight reduction in the silicon content was observed in the sample containing 30% PPR (30s1n1) after the chemical attack, a change not identified in the sample without residue. Baščarević et al. [49] reported that sulfate attacks target the Si-O-Si bonds within the aluminosilicate gel structure. Since incorporating PPR increases the silicon content, the residue may have made this sample more susceptible to attack than the geopolymer without residue.

Another noteworthy aspect is the significant increase in magnesium content. Although both metakaolin and PPR contain trace amounts of magnesium oxide, the quantity present in the non-attacked samples was insufficient to be detected by chemical analysis. Therefore, the likely source of the magnesium is the magnesium sulfate solution used in the experiment. Magnesium was identified; thus, forming magnesium aluminosilicate gel (M-A-S-H) is suggested as a possibility. Long et al. [18] found that M-A-S-H gel had formed in fly ash-based geopolymeric concrete after exposure to magnesium sulfate attack, supported by XRD, FTIR, SEM-EDS analysis, and the findings of Ismail et al. [50] and Zawrah et al. [51], Aiken et al. [52].

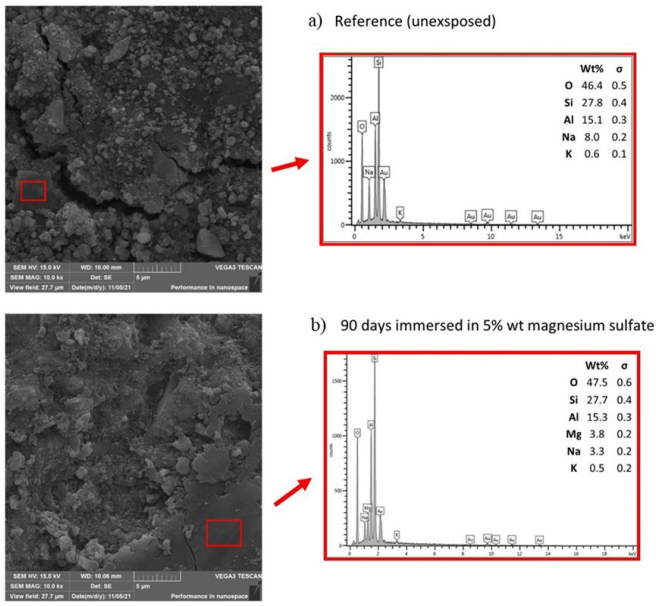

Figure 9. SEM-EDS of the 0n1s1 geopolymer a) reference (unexposed) and b) 90 days immersed in 5% wt magnesium sulfate.

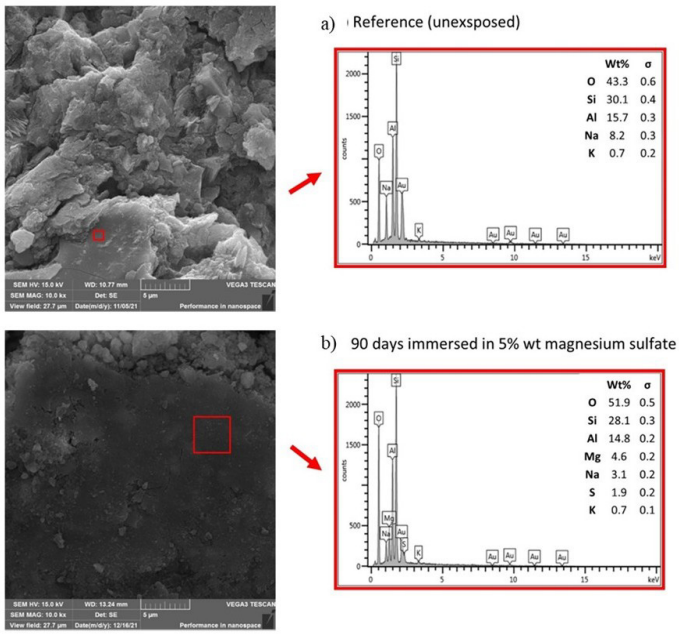

Figure 10. SEM-EDS of the 30n1s1 geopolymer a) reference (unexposed) and b) 90 days immersed in 5% wt magnesium sulfate.

3.2.4 Thermal analysis

Figure 11-a shows the thermogravimetric and differential thermal analysis curves for the n1s1 group reference geopolymer (unexposed), and Figure 11-b shows the results of the samples after the magnesium sulfate attack. In Figure 11-a the greatest mass loss occurred in the sample without residue, being reduced as a function of the increase in residue content, so that the sample with the highest percentage of PPR (45%), showed the smallest reduction. Similarly, the largest fraction of losses was recorded between 100°C and 250°C, attributed to the loss of free and chemically bound water in the system [51], [52]. The slight variations observed between 450°C and 700°C are associated with the decomposition of carbonates [50]. Such losses seem to stabilize by following the DTG curve, close to the values of 800°C-850°C.

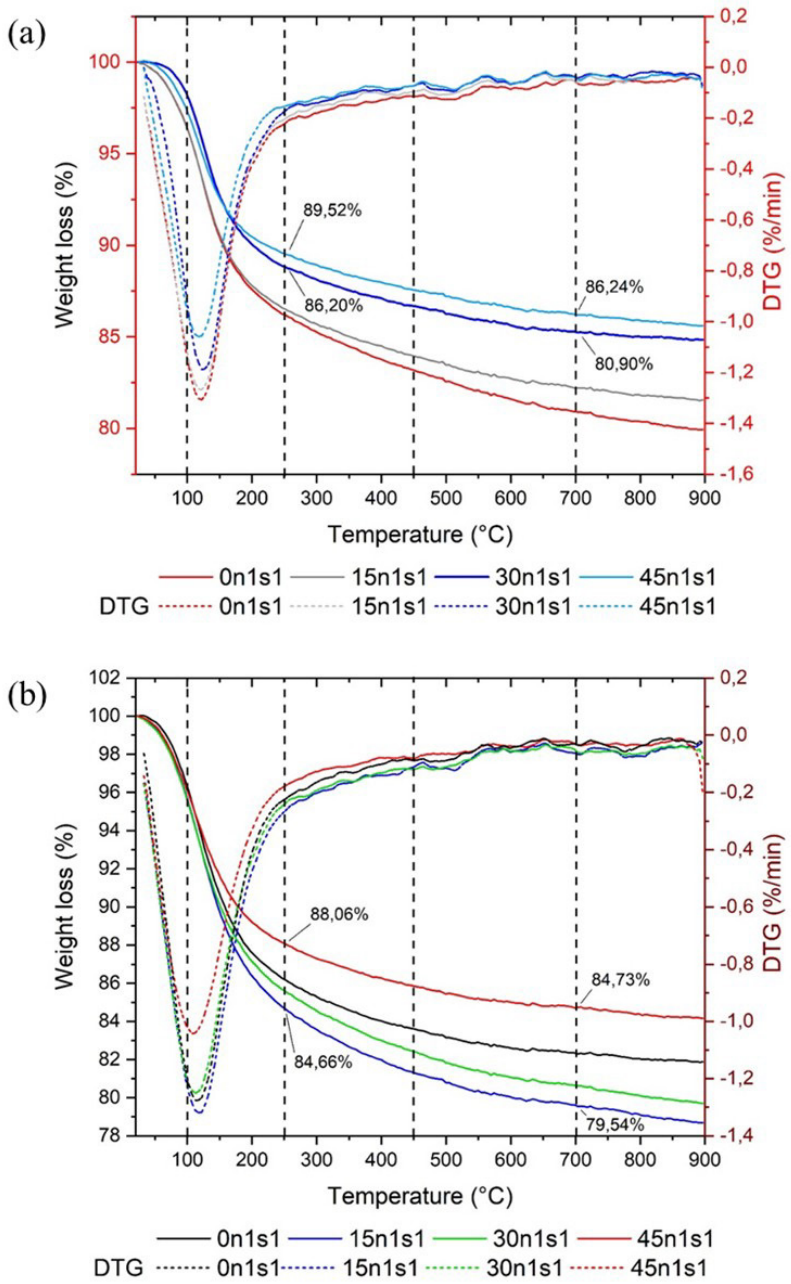

Figure 11. Thermogravimetric curves of (a) reference and (b) samples immersed in 5 wt% sulfate magnesium of n1s1 group reference geopolymers.

Concerning the samples attacked by magnesium sulfate (Figure 11-b), similar mass losses to the reference samples were recorded, in the range of 16 and 21%, also evidencing the stability of geopolymeric samples against sulfate attack. The sample with 15% residue registered the greatest mass loss (15n1s1), preceded by the sample with 30%, 0%, and 45%. Thus, it can be seen that the highest PPR content (45%) continued to show greater stability, despite the samples with 15% and 30% having had greater mass loss than the sample without residue. As the SEM-EDS analyses demonstrated, in the sulfate attack, the migration of the Mg^{2+} cation in the geopolymeric matrix was observed, which acted as network modifier cations [17], binding to the aluminosilicate gel, resulting in the formation of magnesium aluminosilicate gels (M-A-S-H), similar in nature to the N-A-S-H gel [18]. So, it is considered that some of these reactions associated with ion exchange and/or adhesion of Mg^{2+} to the geopolymer reaction product allowed samples without residue to generate a phase that is more resistant to the effect of temperature [53]. This behavior is complemented by the significant increase in compressive strength (see section 3.2.5) after exposure to sulfate. It should be noted that this phase does not differ significantly from the N-A-S-H since, by viewing the DTG, they have similar thermal behavior [17], [18].

3.3 Compressive Strength

The compressive strength values of the geopolymeric compositions without exposure to the sulfate solution (Reference) and after 30, 60, and 90 days of exposure are presented in Figure 12-a, along with the percentage increases observed compared to the respective references, as shown in Figure 12-b. As can be observed, for all evaluated PPR contents and precursor proportions, increases in mechanical properties were noted, with this increase being proportional to the exposure time; i.e., the longer the exposure period, the greater the observed increment. Bakharev [17] observed a 35% and 12% increase in the compressive strength of geopolymeric cement pastes based on FA after the samples were immersed in a 5 wt% magnesium sulfate solution for 6 months. According to the author, this increase in strength is attributed to the migration of Mg^{2+} cations into the geopolymeric matrix, confirmed through SEM-EDS analysis of the affected matrix and Inductively Coupled Plasma Optical Emission Spectrometry and Ion Chromatography (ICP-OES/IC) of the sulfate solution. Based on Bakharev's findings [17], the migrated Mg^{2+} ions likely acted as network modifiers by binding to the aluminosilicate gel, thereby enhancing the compressive strength of the samples. Long et al. [18], while conducting a chemical attack in a 5 wt% magnesium sulfate solution on fly ash-based geopolymeric cement concrete samples activated with an alkaline silicate solution and sodium hydroxide, observed a 72% increase in compressive strength at the end of the exposure period. The sulfate attack involved 32 cycles/day of wetting and drying, consisting of continuous immersion of the samples for 14 hours at 20°C, followed by drying at 80°C for 5 hours, and then another 5 hours at 20°C, totaling 24 hours per cycle. Through microstructural analyses using XRD, FTIR, and SEM-EDS, the authors attributed the significant increase in compressive strength to the migration of Mg^{2+} cations into the matrix, which led to the formation of magnesium aluminosilicate gels (M-A-S-H), similar in nature to the geopolymerization reaction product gel (N-A-S-H)

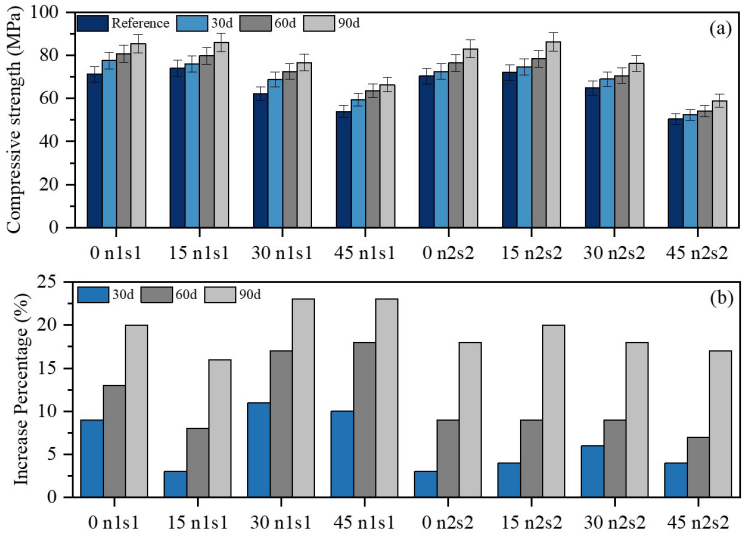

Figure 12. Compressive strength (a) and increase percentage (b) of geopolymeric samples subjected to magnesium sulfate attack.

Thus, it was identified in the work of Bakharev [17] and Long et al. [18] several similarities with this research, both regarding the test conditions (same type of cement, same sulfate, and same concentration) and concerning the microstructural results, especially the chemical analysis carried out by SEM-EDS, which confirmed the presence of Mg^{2+} from the sulfate solution to the geopolymer matrix. Therefore, given the increase in the compressive strength of the samples and the considerations of these works, it is assumed that the attack by magnesium sulfate triggered the migration of Mg^{2+}, which acted as a network modifier cation, binding itself to the aluminosilicate gel and forming the M-A-S-H gel, which favored the compressive strength of the samples between 16 to 23%.

4 CONCLUSIONS

The following conclusions were reached based on the durability assessment of binary geopolymers composed of MK and PPR submitted to magnesium sulfate attack up to 90 days of exposure:

- Visual inspection of the specimens after 90 days of exposure to the sulfate solution revealed no signs of cracking or efflorescence, indicating the effective performance of the geopolymeric matrices against magnesium sulfate.
- The gradual increase in MK substitution with PPR led to compressive strength reductions of up to 28% in the geopolymers, attributed to the lower reactivity of PPR. This is further supported by the reduced formation of N-A-S-H in PPR-containing samples, as confirmed by quantitative XRD analysis.
- Identified Mg^{2+} cation migration is associated with the formation of magnesium aluminosilicate gels (M-A-S-H), similar in nature to the polymerization reaction product (N-A-S-H), explaining the increase in the 20% range of compressive strength that the samples had.

In summary, this research contributes valuable insights into the durability of geopolymeric materials against sulfate attack, highlighting their potential for sustainability. The study demonstrates the feasibility of using an alternative binder with reduced environmental impact, incorporating up to 30% PPR— a waste material lacking a well-established disposal method. The results also confirmed the superior durability of geopolymeric cements, which remained stable in sulfate-rich aggressive environments. Overall, the findings underscore the potential for broader application of geopolymeric cements.

This study has some limitations, e.g., porosimetry tests were not conducted, which could provide valuable insights into the pore network and its influence on sulfate resistance. Additionally, the exposure period was limited to 90 days, so longer-term durability and performance under other aggressive or real-world exposure conditions still need to be investigated. Future work should include detailed pore structure analyses and extended testing periods to better understand degradation mechanisms. Furthermore, exploring other industrial residues as partial replacements and optimizing mix designs could further enhance the potential of these geopolymer materials for sustainable construction.

ACKNOWLEDGEMENTS

The authors acknowledged the Brazilian research agencies National Council for Scientific and Technological Development (CNPq), Coordination for the Improvement of Higher Education Personnel (CAPES), and Santa Catarina Research Foundation (FAPESC). Additionally, we acknowledged LABMAT (UFSC), LDRX (UFSC), and LCP (UFSC). L.S. acknowledges Fundação Araucária for her productivity grant.

REFERENCES

[1] K. L. Scrivener, V. M. John, and E. M. Gartner, "Eco-efficient cements: potential economically viable solutions for a low-CO2 cement-based materials industry," *Cement Concr. Res.*, vol. 114, pp. 2–26, 2018, http://doi.org/10.1016/j.cemconres.2018.03.015.

[2] International Energy Agency, *Low-Carbon Transition in the Cement Industry: Technology Roadmap*. Paris: IEA, 2018.

[3] A. Valero, A. Agudelo, and A. Valero, "The crepuscular planet. A model for the exhausted atmosphere and hydrosphere," *Energy*, vol. 36, no. 6, pp. 3745–3753, 2011, http://doi.org/10.1016/j.energy.2010.07.017.

[4] K. C. Seto, B. Güneralp, and L. R. Hutyra, "Global forecasts of urban expansion to 2030 and direct impacts on biodiversity and carbon pools," *Proc. Natl. Acad. Sci. USA*, vol. 109, no. 40, pp. 16083–16088, 2012, http://doi.org/10.1073/pnas.1211658109. PMid:22988086.

[5] B. Mather, "Concrete durability," *Cement Concr. Compos.*, vol. 26, no. 1, pp. 3–4, 2004, http://doi.org/10.1016/S0958-9465(02)00122-1.

[6] F. Pacheco-Torgal, J. Castro-Gomes, and S. Jalali, "Alkali-activated binders: A review. Part 2. About materials and binders manufacture," *Constr. Build. Mater.*, vol. 22, no. 7, pp. 1315–1322, 2008, http://doi.org/10.1016/j.conbuildmat.2007.03.019.

[7] P. Chindaprasirt and U. Rattanasak, "Improvement of durability of cement pipe with high calcium fly ash geopolymer covering," *Constr. Build. Mater.*, vol. 112, pp. 956–961, 2016, http://doi.org/10.1016/j.conbuildmat.2016.03.023.

[8] H. A. Khan, M. S. H. Khan, A. Castel, and J. Sunarho, "Deterioration of alkali-activated mortars exposed to natural aggressive sewer environment," *Constr. Build. Mater.*, vol. 186, pp. 577–597, 2018, http://doi.org/10.1016/j.conbuildmat.2018.07.137.

[9] P. Sturm, G. J. G. Gluth, C. Jäger, H. J. H. Brouwers, and H.-C. Kühne, "Sulfuric acid resistance of one-part alkali-activated mortars," *Cement Concr. Res.*, vol. 109, pp. 54–63, 2018, http://doi.org/10.1016/j.cemconres.2018.04.009.

[10] A. Neville, "The confused world of sulfate attack on concrete," *Cement Concr. Res.*, vol. 34, no. 8, pp. 1275–1296, 2004, http://doi.org/10.1016/j.cemconres.2004.04.004.

[11] S. W. Tang, Y. Yao, C. Andrade, and Z. J. Li, "Recent durability studies on concrete structure," *Cement Concr. Res.*, vol. 78, pp. 143–154, 2015, http://doi.org/10.1016/j.cemconres.2015.05.021.

[12] P.K. Mehta and P.J.M. Monteiro, *Concrete: Microstructures, Properties, and Materials*, New York: McGraw-Hill, 2014.

[13] J. Kwasny, T. A. Aiken, M. N. Soutsos, J. A. McIntosh, and D. J. Cleland, "Sulfate and acid resistance of lithomarge-based geopolymer mortars," *Constr. Build. Mater.*, vol. 166, pp. 537–553, 2018, http://doi.org/10.1016/j.conbuildmat.2018.01.129.

[14] A. Garg, D. Singhal, and Parveen, "Parveen, Review on the durability properties of sustainable alkali activated concrete," *Mater. Today Proc.*, vol. 33, pp. 1643–1649, 2020, http://doi.org/10.1016/j.matpr.2020.06.370.

[15] T. Bakharev, "Resistance of geopolymer materials to acid attack," *Cement Concr. Res.*, vol. 35, no. 4, pp. 658–670, 2005, http://doi.org/10.1016/j.cemconres.2004.06.005.

[16] M. Albitar, M. S. Mohamed Ali, P. Visintin, and M. Drechsler, "Durability evaluation of geopolymer and conventional concretes," *Constr. Build. Mater.*, vol. 136, pp. 374–385, 2017, http://doi.org/10.1016/j.conbuildmat.2017.01.056.

[17] T. Bakharev, "Durability of geopolymer materials in sodium and magnesium sulfate solutions," *Cement Concr. Res.*, vol. 35, no. 6, pp. 1233–1246, 2005, http://doi.org/10.1016/j.cemconres.2004.09.002.

[18] T. Long, Q. Wang, Z. Guan, Y. Chen, and X. Shi, "Deterioration and microstructural evolution of the fly ash geopolymer concrete against MgSO 4 solution," *Adv. Mater. Sci. Eng.*, vol. 2017, pp. 1–11, 2017, http://doi.org/10.1155/2017/4247217.

[19] L. B. de Oliveira, A. R. G. de Azevedo, M. T. Marvila, E. C. Pereira, R. Fediuk, and C. M. F. Vieira, "Durability of geopolymers with industrial waste," *Case Stud. Constr. Mater.*, vol. 16, pp. e00839, 2022, http://doi.org/10.1016/j.cscm.2021.e00839.

[20] H. E. Elyamany, A. E. M. Abd Elmoaty, and A. M. Elshaboury, "Magnesium sulfate resistance of geopolymer mortar," *Constr. Build. Mater.*, vol. 184, pp. 111–127, 2018, http://doi.org/10.1016/j.conbuildmat.2018.06.212.

[21] Z. Deng and Z. Deng, "Short-term improvement of ductile geopolymer composites exposed to magnesium sulfate: Mechanical properties, sorptivity, and mechanisms," *Constr. Build. Mater.*, vol. 408, pp. 133648, 2023, http://doi.org/10.1016/j.conbuildmat.2023.133648.

[22] R. P. Singh, K. R. Vanapalli, K. Jadda, and B. Mohanty, "Durability assessment of fly ash, GGBS, and silica fume based geopolymer concrete with recycled aggregates against acid and sulfate attack," *J. Build. Eng.*, vol. 82, pp. 108354, 2024, http://doi.org/10.1016/j.jobe.2023.108354.

[23] N. A. M. Beltrame, V. L. Kudlanvec Jr., R. Souto, A. V. Trisotto, J. C. N. da Silva, and R. A. de Medeiros-Junior, "Sulfate attack on geopolymer: effect of the proportion of binder and air-entraining additive," *Rev. IBRACON Estrut. Mater.*, vol. 17, no. 1, pp. 1–14, 2024, http://doi.org/10.1590/s1983-41952024000100014.

[24] A. V. Trisotto, T. A. de Oliveira, M. D. Marçon, N. A. M. Beltrame, and R. A. de Medeiros-Junior, "Effect of carbonation curing and sodium content on geopolymer subjected to sodium and magnesium sulfate attack," *Rev. IBRACON Estrut. Mater.*, vol. 18, no. 1, pp. 1–16, 2025, http://doi.org/10.1590/s1983-41952025000800007.

[25] J. Davidovits, "Geopolymers: inorganic polymeric new materials," *J. Therm. Anal. Calorim.*, vol. 37, no. 8, pp. 1633–1656, 1991, http://doi.org/10.1007/BF01912193.

[26] Z. Sun et al., "Synthesis and thermal behavior of geopolymer-type material from waste ceramic," *Constr. Build. Mater.*, vol. 49, pp. 281–287, 2013, http://doi.org/10.1016/j.conbuildmat.2013.08.063.

[27] G. A. Ramos, P. R. de Matos, F. Pelisser, and P. J. P. Gleize, "Effect of porcelain tile polishing residue on eco-efficient geopolymer: Rheological performance of pastes and mortars," *J. Build. Eng.*, vol. 32, pp. 101699, 2020, http://doi.org/10.1016/j.jobe.2020.101699.

[28] M. Jin, Z. Zheng, Y. Sun, L. Chen, and Z. Jin, "Resistance of metakaolin-MSWI fly ash based geopolymer to acid and alkaline environments," *J. Non-Cryst. Solids*, vol. 450, pp. 116–122, 2016, http://doi.org/10.1016/j.jnoncrysol.2016.07.036.

[29] M. Zhang, M. Zhao, G. Zhang, D. Mann, K. Lumsden, and M. Tao, "Durability of red mud-fly ash based geopolymer and leaching behavior of heavy metals in sulfuric acid solutions and deionized water," *Constr. Build. Mater.*, vol. 124, pp. 373–382, 2016, http://doi.org/10.1016/j.conbuildmat.2016.07.108.

[30] A. Karthik, K. Sudalaimani, and C. T. Vijayakumar, "Durability study on coal fly ash-blast furnace slag geopolymer concretes with bio-additives," *Ceram. Int.*, vol. 43, no. 15, pp. 11935–11943, 2017, http://doi.org/10.1016/j.ceramint.2017.06.042.

[31] G. Ascensão, M. P. Seabra, J. B. Aguiar, and J. A. Labrincha, "Red mud-based geopolymers with tailored alkali diffusion properties and pH buffering ability," *J. Clean. Prod.*, vol. 148, pp. 23–30, 2017, http://doi.org/10.1016/j.jclepro.2017.01.150.

[32] R. M. Novais, G. Ascensão, M. P. Seabra, and J. A. Labrincha, "Waste glass from end-of-life fluorescent lamps as raw material in geopolymers," *Waste Manag.*, vol. 52, pp. 245–255, 2016, http://doi.org/10.1016/j.wasman.2016.04.003. PMid:27067423.

[33] L. Silvestro, T. P. Scolaro, A. S. Ruviaro, G. T. dos Santos Lima, P. J. P. Gleize, and F. Pelisser, "Use of biomass wood ash to produce sustainable geopolymeric pastes," *Constr. Build. Mater.*, vol. 370, pp. 130641, 2023, http://doi.org/10.1016/j.conbuildmat.2023.130641.

[34] A. S. Ruviaro et al., "Valorization of oat husk ash in metakaolin-based geopolymer pastes," *Constr. Build. Mater.*, vol. 367, pp. 130341, 2023, http://doi.org/10.1016/j.conbuildmat.2023.130341.

[35] G. A. Ramos, F. Pelisser, P. J. Paul Gleize, A. M. Bernardin, and M. D. Michel, "Effect of porcelain tile polishing residue on geopolymer cement," *J. Clean. Prod.*, vol. 191, pp. 297–303, 2018, http://doi.org/10.1016/j.jclepro.2018.04.236.

[36] P. R. de Matos, J. S. Andrade Neto, R. D. Sakata, A. P. Kirchheim, E. D. Rodríguez, and C. E. M. Campos, "Strategies for XRD quantitative phase analysis of ordinary and blended Portland cements," *Cement Concr. Compos.*, vol. 131, pp. 104571, 2022, http://doi.org/10.1016/j.cemconcomp.2022.104571.

[37] P. Sukontasukkul, D. Intarabut, T. Phoo-ngernkham, C. Suksiripattanapong, H. Zhang, and P. Chindaprasirt, "Self-compacting steel fibers reinforced geopolymer: Study on mechanical properties and durability against acid and chloride attacks," *Case Stud. Constr. Mater.*, vol. 19, pp. e02298, 2023, http://doi.org/10.1016/j.cscm.2023.e02298.

[38] A. G. Noor Abbas, F. Nora Aznieta Abdul Aziz, K. Abdan, N. Azline Mohd Nasir, and G. Fahim Huseien, "Experimental study on durability properties of kenaf fibre-reinforced geopolymer concrete," *Constr. Build. Mater.*, vol. 396, pp. 132160, 2023, http://doi.org/10.1016/j.conbuildmat.2023.132160.

[39] American Society for Testing and Materials, *Standard Practice for Use of Unbonded Caps in Determination of Compressive Strength of Hardened Cylindrical Concrete Specimens*, ASTM C1231/C1231M-15, 2015.

[40] P. R. de Matos, J. S. Andrade Neto, D. Jansen, A. G. De la Torre, A. P. Kirchheim, and C. E. M. Campos, "In-situ laboratory X-ray diffraction applied to assess cement hydration," *Cement Concr. Res.*, vol. 162, pp. 106988, 2022, http://doi.org/10.1016/j.cemconres.2022.106988.

[41] N. V. Y. Scarlett and I. C. Madsen, "Quantification of phases with partial or no known crystal structures," *Powder Diffr.*, vol. 21, no. 4, pp. 278–284, 2006, http://doi.org/10.1154/1.2362855.

[42] M. Zerzouri Lakhssassi, S. Alehyen, M. El Alouani, and M. Taibi, "The effect of aggressive environments on the properties of a low calcium fly ash based geopolymer and the ordinary Portland cement pastes," *Mater. Today Proc.*, vol. 13, pp. 1169–1177, 2019, http://doi.org/10.1016/j.matpr.2019.04.085.

[43] Z. Makhloufi, S. Aggoun, B. Benabed, E. H. Kadri, and M. Bederina, "Effect of magnesium sulfate on the durability of limestone mortars based on quaternary blended cements," *Cement Concr. Compos.*, vol. 65, pp. 186–199, 2016, http://doi.org/10.1016/j.cemconcomp.2015.10.020.

[44] I. Sirisawat, W. Saengsoy, L. Baingam, P. Krammart, and S. Tangtermsirikul, "Durability and testing of mortar with interground fly ash and limestone cements in sulfate solutions," *Constr. Build. Mater.*, vol. 64, pp. 39–46, 2014, http://doi.org/10.1016/j.conbuildmat.2014.04.083.

[45] S. O. Sore, A. Messan, E. Prud'homme, G. Escadeillas, and F. Tsobnang, "Synthesis and characterization of geopolymer binders based on local materials from Burkina Faso – Metakaolin and rice husk ash," *Constr. Build. Mater.*, vol. 124, pp. 301–311, 2016, http://doi.org/10.1016/j.conbuildmat.2016.07.102.

[46] A. S. Ruviaro, L. Silvestro, H. A. Santana, A. Araújo, and F. Pelisser, "Ternary sustainable geopolymer matrices containing metakaolin, water treatment sludge, and porcelain tile polishing residue," *Constr. Build. Mater.*, vol. 440, pp. 137412, 2024, http://doi.org/10.1016/j.conbuildmat.2024.137412.

[47] E. Álvarez-Ayuso et al., "Environmental, physical and structural characterisation of geopolymer matrixes synthesised from coal (co-)combustion fly ashes," *J. Hazard. Mater.*, vol. 154, no. 1-3, pp. 175–183, 2008, http://doi.org/10.1016/j.jhazmat.2007.10.008. PMid:18006153.

[48] W. Song, T. Guo, P. Han, X. Wang, F. Ma, and B. He, "Durability study and mechanism analysis of red mud-coal metakaolin geopolymer concrete under a sulfate environment," *Constr. Build. Mater.*, vol. 409, pp. 133990, 2023, http://doi.org/10.1016/j.conbuildmat.2023.133990.

[49] Z. Baščarević, M. Komljenović, Z. Miladinović, V. Nikolić, N. Marjanović, and R. Petrović, "Impact of sodium sulfate solution on mechanical properties and structure of fly ash based geopolymers," *Mater. Struct.*, vol. 48, no. 3, pp. 683–697, 2015, http://doi.org/10.1617/s11527-014-0325-4.

[50] I. Ismail, S. A. Bernal, J. L. Provis, S. Hamdan, and J. S. J. van Deventer, "Microstructural changes in alkali activated fly ash/slag geopolymers with sulfate exposure," *Mater. Struct.*, vol. 46, no. 3, pp. 361–373, 2013, http://doi.org/10.1617/s11527-012-9906-2.

[51] M. F. Zawrah, S. E. Abo Sawan, R. M. Khattab, and A. A. Abdel-Shafi, "Effect of nano sand on the properties of metakaolin-based geopolymer: Study on its low rate sintering," *Constr. Build. Mater.*, vol. 246, pp. 118486, 2020, http://doi.org/10.1016/j.conbuildmat.2020.118486.

[52] T. A. Aiken, J. Kwasny, W. Sha, and M. N. Soutsos, "Effect of slag content and activator dosage on the resistance of fly ash geopolymer binders to sulfuric acid attack," *Cement Concr. Res.*, vol. 111, pp. 23–40, 2018, http://doi.org/10.1016/j.cemconres.2018.06.011.

[53] D. Yan, S. Chen, J. Jin, X. Zhu, J. Wang, and Q. Zeng, "Chemical–physical–mechanical stability of MKG mortars under sulfate attacks," *Adv. Cement Res.*, vol. 33, no. 5, pp. 224–238, 2021, http://doi.org/10.1680/jadcr.19.00094.

Author contributions: Giovanny A. Ramos: Conceptualization, Methodology, Investigation, Formal analysis, Writing - original draft. Rafael Dors Sakata: Methodology, Writing – XRD analysis. Laura Silvestro: Formal analysis, Writing - review & editing. Fernando Pelisser: Investigation, Formal analysis, Supervision, Writing - review & editing. Carlos Eduardo Maduro de Campos: Supervision – XRD analysis.

Editors: Edna Possan, Daniel Cardoso.